Springer Mineralogy

Yuriy Litvin
Oleg Safonov *Editors*

# Advances in Experimental and Genetic Mineralogy

## Special Publication to 50th Anniversary of DS Korzhinskii Institute of Experimental Mineralogy of the Russian Academy of Sciences

Springer

Yuriy Litvin · Oleg Safonov
Editors

# Advances in Experimental and Genetic Mineralogy

## Special Publication to 50th Anniversary of DS Korzhinskii Institute of Experimental Mineralogy of the Russian Academy of Sciences

Springer

*Editors*
Yuriy Litvin
Mantle Laboratory
DS Korzhinskii Institute
of Experimental Mineralogy
Russian Academy of Sciences
Chernogolovka, Moscow Oblast, Russia

Oleg Safonov
Metamorphism Laboratory
DS Korzhinskii Institute
of Experimental Mineralogy
Russian Academy of Sciences
Chernogolovka, Moscow Oblast, Russia

ISSN 2366-1585 ISSN 2366-1593 (electronic)
Springer Mineralogy
ISBN 978-3-030-42858-7 ISBN 978-3-030-42859-4 (eBook)
https://doi.org/10.1007/978-3-030-42859-4



This Springer imprint is published by the registered company Springer Nature Switzerland AG
The registered company address is: Gewerbestrasse 11, 6330 Cham, Switzerland

# Contents

# Abbreviations

| | |
|---|---|
| Ab | Albite $NaAlSi_3O_8$ |
| Alm | Almandine $Fe_3Al_2Si_3O_{12}$ |
| An | Anorthite $CaAl_2Si_2O_8$ |
| Ancl | Anorthoclase $(Na, K)AlSi_3O_8$ |
| And | Andalusite $Al_2SiO_5$ |
| Brd | Bridgmanite $MgSiO_3$ |
| CaPrv | Ca-perovskite $CaSiO_3$ |
| Carb, Carb* | Assembly of several carbonates |
| Chr | Chromite $FeCr_2O_4$ |
| Coe | Coesite $SiO_2$ |
| Cpx | Clinopyroxene $(Ca, Na)(Mg, Fe)(Si, Al)_2O_6$; $[(Di{\cdot}Hd{\cdot}Jd)_{ss}]$ |
| Crn | Corundum $Al_2O_3$ |
| D | Diamond C |
| Di | Diopside $CaMgSi_2O_6$ |
| Dol | Dolomite $CaMg(CO_3)_2$ |
| En | Enstatite $MgSiO_3$ |
| Fa | Fayalite $Fe_2SiO_4$ |
| FBrd | Ferrobridgmanite $(Mg, Fe)SiO_3$ |
| Fo | Forsterite $Mg_2SiO_4$ |
| FPer | Ferropericlase $(Mg, Fe)O$ |
| FRwd | Ferroringwoodite $(Mg, Fe)_2SiO_4$ |
| Fs | Ferrosilite $FeSiO_3$ |
| Gros | Grossularite $Ca_3Al_2Si_3O_{12}$ |
| Grt | Garnet $(Mg, Fe, Ca)_3(Al,Cr)_2Si_3O_{12}$; $[(Prp{\cdot}Alm{\cdot}Gros)_{ss}]$ |
| Hd | Hedenbergite $CaFeSi_2O_6$ |
| Jd | Jadeite $NaAlSi_2O_6$ |
| Kfs | K-feldspar $KAlSi_3O_8$ |
| Ky | Kyanite $Al_2SiO_5$ |
| L | Liquid, melt |
| Ma | Mathiasite $(K, Ba, Sr)(Zr, Fe)(Mg, Fe)_2(Ti,Cr,Fe)_{18}O_{38}$ |

| | |
|---|---|
| Mcl | Microlite $NaCaTa_2O_6F$ |
| Mgs | Magnesite $MgCO_3$ |
| Mic | Microcline $KAlSi_3O_8$ |
| MWus | Magnesiowustite (Fe, Mg)O |
| Ol | Olivine $(Mg, Fe)_2SiO_4$; $[(Fo{\cdot}Fa)_{ss}]$ |
| Olg | Oligoclase $(Na, Ca)(Si, Al)_4O_8$ |
| Omph | Omphacite, Jd-rich clinopyroxene |
| Opx | Orthopyroxene $(Mg, Fe)SiO_3$; $[(En{\cdot}Fs)_{ss}]$ |
| Par | Paragonite $NaAl_3Si_3O_{10}(OH)_2$ |
| Pchl | Pyrochlore $(Ca, Na)_2(Nb, Ta)_2O_6(O, OH, F)$ |
| Per | Periclase MgO |
| Pf | Pyrophyllite $Al_2Si_4O_{10}(OH)_2$ |
| Phl | Phlogopite $KMg_3AlSi_3O_{10}(F,OH)_2$ |
| Pl | Plagioclase $(NaAlSi_3O_8{\cdot}CaAl_2Si_2O_8)_{ss}$; $(Ab{\cdot}An)_{ss}$ |
| Pri | Priderite $(K, Ba)(Ti, Fe, Mn)_8O_{16}$ |
| Prp | Pyrope $Mg_3Al_2Si_3O_{12}$ |
| Qz | Quartz $SiO_2$ |
| Rwd | Ringwoodite $Mg_2SiO_4$ |
| Srp | Serpentine $(Mg, Fe, Ni, Al, Zn, Mn)_{2–3}Si_2O_5(OH)_4$ |
| Sti | Stishovite $SiO_2$ |
| Tnt | Tantalite $(Mn, Fe)(Nb, Ta)_2O_6$ |
| Wds | Wadsleyite $Mg_2SiO_4$ |
| Wol | Wollastonite $CaSiO_3$ |
| Wus | Wustite FeO |
| Yim | Yimendite $K(Cr, Ti, Mg, Fe, Al)_{12}O_{19}$ |

## Physical Symbols

| | |
|---|---|
| $A_{Kr}$ | The Krichevskii parameter |
| $f_1^*$ | The pure water fugacity |
| $f_2$ | The fugacity of a solute |
| $G^o(g)$ | The Gibbs energy of a compound in the ideal gas state |
| $G_2^\infty$ | The Gibbs energy of a compound in the state of the standard aqueous solution |
| $K_D$ | The vapor–liquid distribution constant |
| $k_H$ | Henry's constant |
| $m$ | Molality (a number of moles of a substance in 1000 g of water) |
| $N_w \approx 55.508$ | The number of moles of $H_2O$ in 1 kg of water |
| $P_1^*$ | Pressure of saturated water vapor |
| $T_c$ | The critical temperature of pure water |

## Greek Symbols

| | |
|---|---|
| $\rho_c$ | The critical density of pure water |
| $\rho_1^*(L)$ | The pure water density along the liquid side of the saturation vapor–liquid curve |
| $\phi_1^*$ | The fugacity coefficient of pure water |
| $\phi_2^\infty$ | The fugacity coefficient of a solute at infinite dilution in water |

# Chapter 6
# Solubility and Volatility of $MoO_3$ in High-Temperature Aqueous Solutions


**A. V. Plyasunov, T. P. Dadze, G. A. Kashirtseva, and M. P. Novikov**

**Abstract** The thermodynamic properties of the neutral molybdic acid $H_2MoO_4$ are evaluated at 273–623 K and the saturated water vapor pressure from our own solubility data at 563–623 K and literature results at lower temperatures. Combining the Gibbs energies of $H_2MoO_4$ in the state of the aqueous solution with those in the ideal gas state, we calculated Henry's constants and the vapor–liquid distribution constants of $H_2MoO_4$ at 273–623 K, and with the use of the relevant asymptotic relations, extrapolated values of Henry's constants, $k_H$, and vapor–liquid distribution constants, $K_D$, toward the critical point of pure water. Our results show that over the whole temperature range of the existence of the vapor–liquid equilibrium of water, the neutral molybdic acid $H_2MoO_4$ is somewhat less volatile compared with $Si(OH)_4$, and the difference in volatility of these species decreases with the temperature.

**Keywords** Molybdenum trioxide · Molybdic acid · Aqueous solubility · Vapor–liquid distribution · Henry's constant · Krichevskii parameter

## 6.1 Introduction

Since the opening of the Institute of Experimental Mineralogy, one of directions of research here was the study of the solubility of minerals in hydrothermal solutions, with the aim to quantify the transport and deposition of ore minerals. The long list of studied systems and relevant publications is beyond the scope of this contribution, and we will only briefly mention several solubility investigations conducted by the authors of the current research team. These studies include the solubility of amorphous $SiO_2$ in water and in aqueous solutions of acids at 373–673 K and pressure of 101.3 MPa (Sorokin and Dadze 1980), of $SnO_2$ in water and aqueous solutions of acids and salts at 473–673 K and pressure of up to 150 MPa (Dadze et al. 1981; Dadze and Sorokin 1986); the solubility of zinc oxide ZnO in aqueous solutions of alkalis (Plyasunov et al. 1988; Plyasunov and Plyasunova 1993a), salts (Plyasunov and Ivanov 1991)

A. V. Plyasunov (✉) · T. P. Dadze · G. A. Kashirtseva · M. P. Novikov
D.S. Korzhinskii Institute of Experimental Mineralogy, Russian Academy of Sciences, Academician Osipyan Street 4, Chernogolovka, Moscow Region, Russia 142432
e-mail: andrey.plyasunov@gmail.com



Y. Litvin and O. Safonov (eds.), *Advances in Experimental and Genetic Mineralogy*, Springer Mineralogy, https://doi.org/10.1007/978-3-030-42859-4_6

and alkali + salt mixtures (Plyasunov and Plyasunova 1993b) at 473–873 K and pressures up to 200 MPa; investigations of solubility of gold in aqueous $H_2S$-bearing solutions (Dadze et al. 1999, 2000, 2001; Dadze and Kashirtseva 2004; Gorbachev et al. 2010), including solubility in low-density hydrothermal fluids (Zakirov et al. 2008, 2009).

The current contribution is concerned with the thermodynamic properties of the neutral molybdic acid $H_2MoO_4$ (its real stoichiometry is likely $MoO_2(OH)_2$ (Akinfiev and Plyasunov 2013)) in aqueous solutions at elevated temperatures. The primary motivation for this study were the unusual results by Rempel et al. (2009), who studied the vapor–liquid distribution of Mo from $(NH_4)_2MoO_4$ solutions at 573–643 K, and reported that $H_2MoO_4$(aq) is more volatile (in terms of Henry's constants) than, for example, Ar. As the interactions between water and nonpolar Ar are much weaker than those for $H_2MoO_4$, which form hydrogen bonds with $H_2O$ molecules, such finding appears unlikely. However, an earlier publication by Khitarov et al. (1967) on the partition of Mo(VI) from dilute solutions of $Na_2MoO_4$ over a temperature range 523–623 K also found unexpectedly high concentrations of molybdenum in the vapor phase. Such was the situation before the start of our investigation: Mo(VI) compounds appeared to be highly anomalous in terms of their partition from aqueous solutions, challenging our knowledge of regularities in water-solute interactions. Nevertheless, one may speculate that trapping a portion of vapor phase in a two-phase system, as was done in studies (Khitarov et al. 1967; Rempel et al. 2009), is an error-prone method, especially when the incomplete separation of liquid and vapor phases is recognized as one of the major issues in the experimental studies of the vapor–liquid partitioning of aqueous solutes (Palmer et al. 2004). Indeed, in 2016, Kokh et al. (2016) published results of the study, where a direct sampling of the coexisting vapor and liquid phases at 623 K was employed. The liquid phase was ~1 m salt solution, and contained small amounts of Mo and other metals. In the S-free, $CO_2$-free series of experiments concentrations of Mo(VI) in steam were 3–3.5 orders of magnitude lower than in earlier experiments (Khitarov et al. 1967; Rempel et al. 2009).

Existing discrepancies in the Mo vapor–liquid partitioning from aqueous solutions were the main reasons to begin a new study of the distribution of $H_2MoO_4$ between the vapor and liquid phases of water. We have chosen an indirect way to obtain the values of the vapor–liquid distribution constants of the neutral form $H_2MoO_4$. First, we determined the thermodynamic properties of this species from the solubility of molybdite, $MoO_3$, in liquid acid solutions at 563–623 K. Thermodynamic properties of $H_2MoO_4$ in the ideal gas state are already known (Akinfiev and Plyasunov 2013). The difference of the Gibbs energies of this form in the standard aqueous solution and in the ideal gas state gives Henry's constant of $H_2MoO_4$. Henry's constant and the vapor–liquid constant are connected through a relation, which is simple, but requires the knowledge of the fugacity coefficient of the neutral molybdic acid, which can be evaluated, as will be discussed in Sect. 6.3.2.

Over the course of this work, it was found necessary to perform a series of additional experimental investigations for a proper interpretation of the obtained results. First, our studies of the solubility of $MoO_3$ in HCl and $HClO_4$ solutions at an acid molality above 0.03 m showed an increase in the solubility in HCl, but not in $HClO_4$

solutions, indicating the formation of chloride complex(es) of Mo(VI), in agreement with earlier works (Kudrin 1985; Borg et al. 2012). In order to address this issue, we (Dadze et al. 2018b) performed at 573 K and 10 MPa the study of solubility of $MoO_3$ in aqueous solutions of the mixture HCl–$HClO_4$–NaCl (up to 1 m of chloride ion). These data can be explained by the formation of the species $MoO_2(OH)_2Cl^-$, with $\log_{10}K^o = -(0.87 \pm 0.20)$ for the solubility reaction $MoO_3(cr) + H_2O(l) + Cl^- = MoO_2(OH)_2Cl^-$. Second, the thermodynamic interpretation of the solubility values in $Na^+$-bearing solutions may be affected by the formation of the complex species $NaHMoO_4(aq)$, as suggested by Kudrin (1989). Therefore, we (Dadze et al. 2017b) studied, at 573 K and 10 MPa, the solubility of $MoO_3$ in aqueous solutions of $NaClO_4$ up to the salt concentration of 2.21 m, and found no need to invoke a complex formation between $Na^+$ and $HMoO_4^-$, as solubility data could be fully explained by the variations of the activity coefficients of $H^+$ and $HMoO_4^-$ in sodium perchlorate solutions. Finally, we note that at room temperatures the Mo(VI) speciation at the metal concentrations above 0.001 m and pH < 6 is dominated by highly charged polymeric species, containing 6, 7, 8, … up to 36 Mo atoms per polymer (Cruywagen 2000). However, we expect that at high temperatures simple monomeric species will predominate in aqueous Mo-bearing solutions, and such an assumption was explicitly used at interpretation of our $MoO_3$ solubility data. The reason is that highly charged polymers experience an electrostatic repulsion, which has to be overcome when polynuclear species are formed from mononuclear constituents. The high value of the dielectric constant ($\varepsilon \sim 78$ at 298 K) decreases the electrostatic forces at room temperatures, however, the dielectric constant of water falls at high temperatures (for example, at 573 K $\varepsilon \sim 20$), forcing highly charged polynuclear forms to dissociate into monomeric species (Plyasunov and Grenthe 1994) with the increase of temperature. Nevertheless, in order to verify the assumption that only monomers $HMoO_4^-$ and $H_2MoO_4$ dominate speciation of Mo(VI) in weakly acid aqueous solutions at elevated temperatures, we also studied (Dadze et al. 2018a) the solubility of calcium molybdate $CaMoO_4$ (the mineral powellite) at 573 K and 10 MPa in acid (HCl, $HClO_4$) and salt (NaCl, $NaClO_4$) solutions, because the Mo(VI) concentrations at the $CaMoO_4$ solubility are about 10–200 times lower that those at the $MoO_3$ solubility. Modeling the $CaMoO_4$ solubility data using the thermodynamic properties of $HMoO_4^-$ and $H_2MoO_4(aq)$ evaluated from data on dissolution of $MoO_3$, i.e., at much higher contents of dissolved molybdenum, showed a satisfactory agreement of experimental and calculated $CaMoO_4$ solubility values, thus providing an indirect confirmation of our assumption that at 573 K polynuclear forms contribute insignificantly to the material balance of dissolved Mo(VI).

All these auxiliary results are described in corresponding publications (Dadze et al. 2017a, b, 2018a, b) and will not be further addressed here. The current contribution is concerned with the thermodynamic properties of the neutral molybdic acid $H_2MoO_4$ and its volatility from aqueous solutions.

## 6.2 Experimental Methods

### 6.2.1 Materials

Crystals of $MoO_3$ were prepared by the three-stage calcining of ammonium molybdate as described earlier (Dadze et al. 2017a). Calcium molybdate $CaMoO_4$ (the mineral powellite) was synthesized from a mixture of $MoO_3$ and $CaCO_3$ taken in equivalent proportions and heated up to $T = 1473$ K. Both the synthesized molybdite and powellite were hydrothermally treated at 573 K for several days in pure water to remove small particles, edges, defects, etc. $MoO_3$ formed elongated crystals with sizes of 1–50 μm, see SEM photo in Supplemental Information to Dadze et al. (2017a). The typical size of the isometric $CaMoO_4$ crystals used for solubility runs was 10–30 μm, see SEM photo in Dadze et al. (2018a).

X-ray powder diffraction patterns were obtained using copper or cobalt Kα radiation on a Bruker D8 Discovery diffractometer, both before and after the experiments. Scanning electron microscopy (SEM) images using secondary electrons at an accelerating voltage of 20 kV were obtained using Tescan VEGA TS 5130MM equipped with the INCAEnergy EDXS (energy dispersive X-ray spectroscopy) microanalysis system. According to the averaged results of 4 electron microprobe analyses, the Ca:Mo atomic ratio in the synthesized calcium molybdate is equal to (0.981 ± 0.014):1.0.

Aqueous solutions of HCl, $HClO_4$, NaCl, and $NaClO_4$ were prepared from commercial reagents.

### 6.2.2 Experimental Procedure

Experiments were carried out in autoclaves made of the titanium alloy VT-8 of ~22 cm in the length and an internal volume of ~20 $cm^3$. Prior to the experiments, autoclaves were loaded with 20 wt% nitric acid solution with the degree of filling of 0.72 and kept for a day at 573 K to produce a protective $TiO_2$ layer (Dadze et al. 2017a). The autoclaves were placed in a vertical cylindrical furnace during the experiments. The temperature gradients were less than 2 K along the autoclave in the case of a typical loading of 10 autoclaves per furnace. A temperature controller Miniterm-300 was used to monitor the temperature to an accuracy of ±1–2 K. Temperature was measured with a type K (chromel-alumel) thermocouple using a multilogger thermometer HH506RA (OMEGA Engineering). Temperature variations during the experiments were typically within ±2 K. The pressure in the autoclaves was not directly measured, but determined by the degree of the filling of the autoclave with a solution. Preliminary experiments showed poor reproducibility at the two-phase (liquid + vapor) conditions. Therefore, in order to avoid the vapor phase in the experimental vessel, the experiments were performed at pressures slightly exceeding the vapor pressure of water at a given temperature. The degree of filling was typically chosen

to slightly exceed the density of liquid water at saturation at a given temperature. The necessary values of the densities of water were calculated using the Wagner and Pruß (2002) equation of state for water. Recommendations for NaCl solutions by Archer (1992) and for $NaClO_4$ solutions by Abdulagatov and Azizov (2003) were applied. Densities of dilute (0.2 m and less) solutions of HCl and $HClO_4$ were assumed to be equal to densities of NaCl solutions of the same molality.

A weighed quantity of crystalline $MoO_3$ (~100 mg) was placed in a titanium container, which was suspended in the upper part of the autoclave in such a way that it did not contact the liquid solution unless the latter expanded up to 95% of the volume of the autoclave. Due to this design, the solid phase was never in contact with the quenched solution. The volume of the added solution was within 12–16 $cm^3$. After the run, the autoclaves were cooled down to room temperature under running cold water for 5–7 min. The time to reach the steady-state for studies involving $MoO_3$ was estimated to be 10–15 h, and for runs with $CaMoO_4$—4 to 7 days, based on a series of kinetic runs at 573 K and 10 MPa, see Dadze et al. (2017a, 2018a).

#### 6.2.2.1 Stability of Dilute Aqueous Perchlorate Solutions

Experiments were performed in dilute (not more than 0.22 m) aqueous solutions of perchloric acid, $HClO_4$. It is well known that concentrated aqueous solutions of perchloric acid decompose when heated above 523 K according to the reaction $H^+ + ClO_4^- = 0.5\ Cl_2 + 0.5\ H_2O + 1.75\ O_2$ (Henderson et al. 1971). Experiments of Henderson et al. (1971) in a titanium reactor showed that rates of decomposition depend strongly on initial $HClO_4$ concentrations, decreasing by more than 2 orders of magnitude with the decreasing molality of perchloric acid from ~4.6 to ~1.0 m. For every 10 K decrease in temperature, the rate of decomposition decreases approximately three-fold. However, the decomposition is negligibly small for 0.2 m acid at 573 K for experiments of a one-day duration (Henderson et al. 1971). In our experiments, the 0.011 m solution of perchloric acid (no solid phase present) with the initial $pH = 1.98 \pm 0.03$ did not show any change of pH values, within errors of measurements, after being held at 573 K and 10 MPa (no vapor phase present) for 1–3 days. In contrast, a decomposition of aqueous $HClO_4$ was detected at 623 K. In blank runs (no solid phase present) of a one-day duration, a strong odor of chlorine from the quenched solution containing initially 0.10 m $HClO_4$ was detected. The pH value of the quenched solution increased from the initial value of 1.04 to 1.43, indicating significant decomposition of $HClO_4$. At the same temperature (623 K) in the quenched solution initially containing 0.01 m perchloric acid, no chlorine odor was detected, and the pH value of the quenched solution corresponded to that of the initial solution, $pH = 2.03$. In contrast, dilute aqueous HCl solutions are stable up to very high (magmatic) temperatures.

### 6.2.3 Chemical Analyses

The molybdenum concentration in quenched solutions after the experiment was determined using the spectrophotometer Spekol-11 at $\lambda = 453$ nm with the thiocyanate method, based on the formation of yellow color thiocyanate complexes of Mo(V) (Marchenko 1971), and by using thiourea as a reducing agent. The detection limit for Mo is 5 μg in a sample, i.e. at the largest aliquot, 10 ml, the minimal measurable molality of Mo is ~$5 \cdot 10^{-6}$ m. At 10 μg of Mo in a sample, the analytical uncertainty is about 20%, and at 20 μg and above—10%. Analytical results at relatively high solubility values (in excess of $10^{-3}$ m) in water and dilute acid solutions were duplicated by the weight loss (WL) method, using the WA-33 (Texma-Robot, Poland) laboratory balance with an accuracy of 0.2 mg. We found a satisfactory agreement of the analytical and WL results on the concentration of molybdenum in the solution (Dadze et al. 2017a, 2018a).

For a few runs with $CaMoO_4$ (Dadze et al. 2018a), analytical concentrations of Ca and Mo have been determined using ICP-MS and/or inductively coupled plasma atomic emission spectrometry (ICP-AES) using a PlasmaQuad II mass spectrometer with a quadrupole mass analyzer (VG Elemental, GB). Independent measurements of Mo concentrations in quenched solutions by either photometry/colorimetry or ICP-MS show a good agreement (within first per cent).

### 6.2.4 Treatment of Experimental Data

The data analysis was carried out using the program OptimA (Shvarov 2015), which processes experimental solubility data to derive the standard Gibbs free energies of specified aqueous complexes. Details of calculations, including corrections for activity coefficients, are described in our publications (Dadze et al. 2017a, b, 2018a, b).

## 6.3 Results and Discussion

### 6.3.1 Solubility Results for $MoO_3$ in Water and Acid Solutions

Experimental results of the solubility of $MoO_3$ in acid solutions, when chloride complexes do not form in appreciable amounts (i.e. at $m$(HCl) < 0.03), are shown in Fig. 6.1 for the most studied isotherm 573 K. As seen, solubility falls with the increase of the acid concentration and can be explained by the formation of two hydroxo complexes of Mo(VI) according to the reactions:

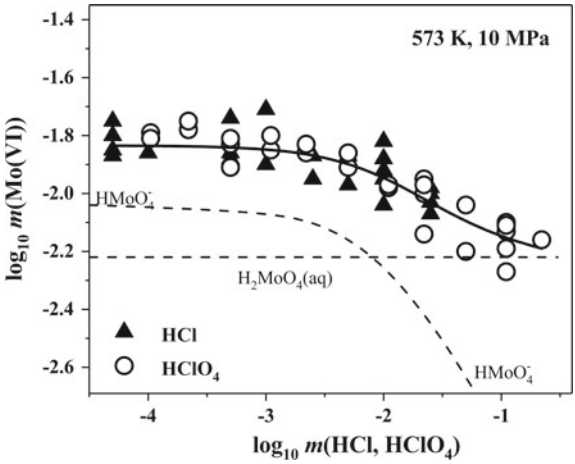


**Fig. 6.1** Solubility of $MoO_3$ in HCl and $HClO_4$ solutions at 573 K, 10 MPa. Symbols designate experimental data, the solid line represents calculated solubility values, while dashed lines shows contributions of $HMoO_4^-$ and $H_2MoO_4$(aq)

$$MoO_3(cr) + H_2O(l) = HMoO_4^- + H^+ \quad (6.1)$$

and

$$MoO_3(cr) + H_2O(l) = H_2MoO_4(aq) \quad (6.2)$$

The most extensive set of data was obtained at 573 K and 10 MPa and it is shown in Fig. 6.1. The following values of $\log_{10}K^o$ have been evaluated from experimental data: $\log_{10}K^o(1)$ −4.25, −4.31, −44.20, −4.55; $\log_{10}K^o(1)$ −2.40, −2.22, −2.41, −1.95 at temperatures 563, 573, 593, 623 K. The expected uncertainty of $\log_{10}K^o$ values is ±0.2 at 563–593 K and may be somewhat higher at 623 K.

In a later publication (Dadze et al. 2018a), we used both our results and the literature values to determine the temperature dependence of equilibrium constants for a number of reactions involving Mo(VI) species (the first and second ionization constants of $H_2MoO_4$, solubility product of powellite $CaMoO_4$, etc.), and to calculate the thermodynamic properties of $H_2MoO_4$(aq), $HMoO_4^-$, and $MoO_4^{2-}$ at 273.15–623 K at the saturated water vapor pressure. The rest of this publication will be concerned with thermodynamic values of the neutral molybdic acid $H_2MoO_4$ in the vapor and liquid phases of water, including recommendations of Henry's constants and vapor–liquid distribution constants over the whole temperature range of existence of the vapor–liquid equilibrium of water, from 273.15 to 647.096 K (the critical temperature of water, $T_c$).

### 6.3.2 *Volatility of $MoO_3$ from Aqueous Solutions*

It is known (Alvarez et al. 1994; Palmer et al. 2004) that overwhelmingly neutral (i.e. non-charged) species partition from aqueous solutions into a vapor phase, as it is energetically very expensive to transfer an ion from a liquid phase into a gas phase that has a much lower value of a dielectric constant. Because of this, the rest of this study will be concerned with the thermodynamic properties of the neutral molybdic acid $H_2MoO_4$. The partition between the liquid and gaseous phases is described by two quantities: the vapor–liquid distribution constant, $K_D$, and Henry's constant, $k_H$. The vapor–liquid distribution constant, $K_D$, is defined as

$$K_D = \lim_{x \to 0} y/x, \tag{6.3}$$

where $y$ and $x$ stand for the mole fractions of a solute in coexisting vapor and liquid phases, respectively. In our case, the simplest way to evaluate $K_D$ is to use the relation between the vapor–liquid distribution constant and Henry's constant, $k_H$, defined as

$$k_H = \lim_{x \to 0} f_2/x, \tag{6.4}$$

where $f_2$ stands for the solute's fugacity. There is a simple relation between two properties (Japas and Levelt Sengers 1989; Alvarez et al. 1994):

$$k_H = \phi_2^\infty \cdot P_1^* \cdot K_D \tag{6.5}$$

where $\phi_2^\infty$ stands for solute's fugacity coefficient at infinite dilution, and $P_1^*$ is the pure solvent pressure at vapor–liquid saturation.

Results of Dadze et al. (2017a) and Akinfiev and Plyasunov (2013), reporting the Gibbs energies of the species $H_2MoO_4$ in the state of an aqueous solution and in the ideal gas state, allow calculating Henry's constants as described below at temperatures between 273 and 623 K at $P_1^*$, see Table 6.1.

The logarithm of Henry's constant is proportional to the difference of the chemical potential of a species in the ideal gas state, $G^o(g)$, and in the state of the standard aqueous solution, $G_2^\infty$:

$$\ln k_H(\text{bar}) = -[G^o(g) - G_2^\infty - RT \ \ln \ N_w]/RT \tag{6.6}$$

and

$$\ln k_H(\text{MPa}) = \ln k_H(\text{bar}) - \ln 10 \tag{6.7}$$

where $N_w \approx 55.508$ is the number of moles of water in 1 kg of water, the last term in Eq. (6.6) is needed because $G_2^\infty$ is in the molality concentration scale, while Henry's constant is in the mole fraction scale.

**Table 6.1** Thermodynamic properties of liquid water (the vapor pressure $P_1^*$, the fugacity $f_1^*$ at $P_1^*$, the density of the liquid water $\rho_1^*(L)$ at $P_1^*$, and of molybdic acid in water, $G_2^\infty$ ($H_2MoO_4$(aq)), and in the ideal gas state $G^o$ ($H_2MoO_4$(g)), Henry's constant, $k_H$, the fugacity coefficient at infinite dilution, $\phi_2^\infty$, the vapor–liquid distribution constant, $K_D$, of molybdic acid in water)

| $T$ (K) | ln $P_1^*$ (MPa)[a] | ln $f_1^*$ (MPa)[a] | $\rho_1^*(L)$ (mol cm$^{-3}$)[a] | $G_2^\infty$ ($H_2MoO_4$(aq)) (kJ mol$^{-1}$)[b] | $G^o$ ($H_2MoO_4$(g)) (kJ mol$^{-1}$)[c] | ln $k_H$ (MPa)[d] | ln $\phi_2^\infty$[e] | ln $K_D$[f] |
|---|---|---|---|---|---|---|---|---|
| 273.15 | −7.400 | −7.401 | 0.055497 | −881.09 | −783.04 | −41.46 | 0.00 | −34.05 |
| 283.15 | −6.702 | −6.703 | 0.055489 | −881.69 | −786.39 | −38.77 | −0.01 | −32.06 |
| 293.15 | −6.058 | −6.059 | 0.055406 | −882.40 | −789.79 | −36.28 | −0.01 | −30.21 |
| 298.15 | −5.754 | −5.756 | 0.055342 | −882.78 | −791.50 | −35.11 | −0.01 | −29.34 |
| 303.15 | −5.462 | −5.463 | 0.055265 | −883.19 | −793.22 | −33.98 | −0.01 | −28.50 |
| 313.15 | −4.908 | −4.911 | 0.055074 | −884.06 | −796.70 | −31.84 | −0.02 | −26.91 |
| 323.15 | −4.394 | −4.398 | 0.054842 | −885.03 | −800.22 | −29.85 | −0.03 | −25.43 |
| 333.15 | −3.915 | −3.920 | 0.054574 | −886.08 | −803.77 | −28.00 | −0.04 | −24.05 |
| 343.15 | −3.467 | −3.474 | 0.054273 | −887.21 | −807.36 | −26.27 | −0.05 | −22.76 |
| 348.15 | −3.255 | −3.263 | 0.054110 | −887.81 | −809.17 | −25.45 | −0.06 | −22.14 |
| 353.15 | −3.049 | −3.058 | 0.053941 | −888.43 | −810.99 | −24.66 | −0.06 | −21.55 |
| 363.15 | −2.657 | −2.669 | 0.053582 | −889.74 | −814.65 | −23.15 | −0.08 | −20.41 |
| 373.15 | −2.289 | −2.304 | 0.053196 | −891.12 | −818.35 | −21.74 | −0.11 | −19.35 |
| 398.15 | −1.460 | −1.486 | 0.052124 | −894.92 | −827.74 | −18.58 | −0.18 | −16.94 |
| 423.15 | −0.742 | −0.783 | 0.050902 | −899.21 | −837.32 | −15.88 | −0.29 | −14.85 |
| 448.15 | −0.114 | −0.174 | 0.049529 | −903.97 | −847.10 | −13.55 | −0.43 | −13.01 |
| 473.15 | 0.441 | 0.355 | 0.047996 | −909.18 | −857.05 | −11.54 | −0.60 | −11.38 |
| 498.15 | 0.936 | 0.819 | 0.046280 | −914.84 | −867.17 | −9.79 | −0.82 | −9.91 |

(continued)

**Table 6.1** (continued)

| $T$ (K) | ln $P_1^*$ (MPa)[a] | ln $f_1^*$ (MPa)[a] | $\rho_1^*(L)$ (mol cm$^{-3}$)[a] | $G_2^\infty$ ($H_2MoO_4$(aq)) (kJ mol$^{-1}$)[b] | $G^o$ ($H_2MoO_4$(g)) (kJ mol$^{-1}$)[c] | ln $k_H$ (MPa)[d] | ln $\phi_2^{\infty}$[e] | ln $K_D$[f] |
|---|---|---|---|---|---|---|---|---|
| 523.15 | 1.380 | 1.227 | 0.044345 | −920.93 | −877.45 | −8.28 | −1.07 | −8.59 |
| 548.15 | 1.783 | 1.588 | 0.042131 | −927.44 | −887.89 | −6.96 | −1.36 | −7.38 |
| 573.15 | 2.150 | 1.908 | 0.039530 | −934.35 | −898.48 | −5.81 | −1.70 | −6.27 |
| 598.15 | 2.489 | 2.193 | 0.036321 | −941.67 | −909.21 | −4.81 | −2.07 | −5.23 |
| 623.15 | 2.805 | 2.448 | 0.031901 | −949.36 | −920.08 | −3.94 | −2.50 | −4.24 |
| 633.15 | 2.927 | 2.542 | 0.029286 | (−950.23) | −924.47 | (−3.18) | (−3.02) | (−3.09) |
| 643.15 | 3.047 | 2.632 | 0.025058 | (−951.09) | −928.88 | (−2.44) | (−3.57) | (−1.92) |
| 647.096 | 3.094 | 2.667 | 0.017874 | (−947.49) | −930.62 | (−1.42) | (−4.51) | 0 |

[a]Wagner and Pruß (2002); [b]Dadze et al. (2018a) at 273.15–623.15 K at $P_1^*$, at 633.15–647.096 K—see text; [c]Akinfiev and Plyasunov (2013); [d]Eqs. (6.6)–(6.7) at 273.15–623.15 K; at 633.15–647.096 K—Eq. (6.10); [e]Eq. (6.8) at 273.15–623.15 K at $P_1^*$, at 633.15–647.096 K—see text; [f]Eq. (6.5) at 273.15–623.15 K, at 633.15–647.096 K—Eq. (6.9)

The relation (6.5) can be used to calculate $K_D$ provided that the values of $\phi_2^\infty$ can be estimated. Elsewhere (Akinfiev and Plyasunov 2013; Dadze et al. 2017a) we recommended for $H_2MoO_4$ the approximation

$$\ln \phi_2^\infty \approx k \cdot \ln \phi_1^* = 7 \cdot \ln \phi_1^*, \tag{6.8}$$

where $\phi_1^*$ is the fugacity coefficient of pure water (Wagner and Pruß 2002), and the rules to estimate $k$ depending on the composition of a compound were discussed in Akinfiev and Plyasunov (2013). It was shown that Eq. (6.8) allows a satisfactory prediction of solubility of $MoO_3$ in steam at 573–873 K at water densities up to ~250 kg $m^{-3}$, see Dadze et al. (2017a) for detail. Values of $K_D$ evaluated with relations (6.5) and (6.8) at 273.15–623.15 K are given in Table 6.1.

#### 6.3.2.1 Extrapolation of $K_D$ and $k_H$ Toward the Critical Point of Water

The value of the vapor–liquid distribution constant at the critical point of water is equal to 1, as the liquid and the vapor phase became indistinguishable here. The question is, what is the law governing the course of $K_D$ toward the critical point of a solvent? This question was solved theoretically by Japas and Levelt Sengers (1989) and confirmed by the reliable data (Fernández-Prini et al. 2003): at temperatures above ~500 K and up to the critical temperature of water, variations of $K_D$ can be quantitatively described by the relation:

$$RT \ln K_D = A_{Kr} \cdot \frac{2\left(\rho_1^*(L) - \rho_c\right)}{\rho_c^2}, \tag{6.9}$$

where $A_{Kr}$ is the Krichevskii parameter, the main thermodynamic characteristic of a solute close to the critical point of a solvent, see Levelt Sengers (1991) for the corresponding discussion; $\rho_c$ stands for the critical density of the solvent (322 kg $m^{-3}$ for water), $\rho_1^*(L)$ is the pure water density along the liquid side of the saturation vapor–liquid curve (note that in order to obtain values of $A_{Kr}$ in MPa, density values should be in $cm^{-3}$ mol). Equation (6.9) was employed by us earlier (Dadze et al. 2017a) to evaluate $A_{Kr} = -228 \pm 33$ MPa for $H_2MoO_4$ in water. The relation (6.9) was used to estimate $K_D$ at 633.15, 643.15 and $T_c$, see values in parentheses in the corresponding column of Table 6.1.

The theoretically-based asymptotic (i.e. valid in the neighborhood of the critical point of a solvent) relation was derived (Japas and Levelt Sengers 1989) for Henry's constant as well

$$RT \ln \frac{k_H}{f_1^*} = C_o + A_{Kr} \cdot \frac{\left(\rho_1^*(L) - \rho_c\right)}{\rho_c^2}, \tag{6.10}$$

The evaluation of the constant $C_o$ for $H_2MoO_4$ can be made in the same way as for $Si(OH)_4$ (Plyasunov 2012), i.e. by plotting the values of the auxiliary function $Z$

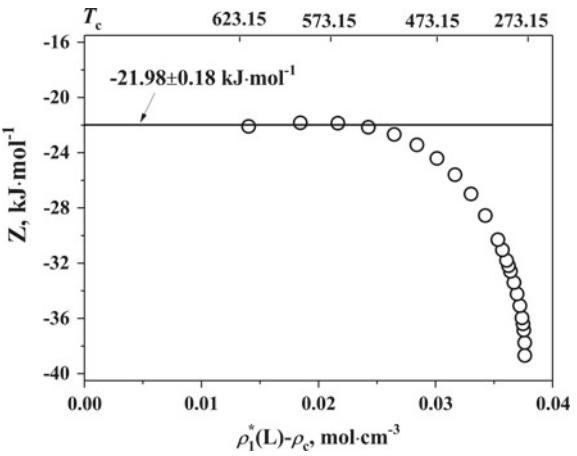


**Fig. 6.2** Evaluation of $C_o$ for $H_2MoO_4$ from $k_H$ data

$$Z = RT\ \ln\frac{k_H}{f_1^*} - A_{\mathrm{Kr}}\cdot\frac{\left(\rho_1^*(L)-\rho_c\right)}{\rho_c^2} \tag{6.11}$$

versus $\rho_1^*(L)-\rho_c$, see Fig. 6.2. According to Eq. (6.10), the auxiliary function $Z$ close to the critical point of water should approach the constant value equal to $C_o$, and data for $H_2MoO_4$ confirm that at temperatures above 550 K with $C_o = -21.98 \pm 0.18$ ($2\sigma$) kJ mol$^{-1}$. With relation (6.10) we estimated $k_H$ at 633.15, 643.15 and $T_c$, see values in parentheses in the corresponding column of Table 6.1.

#### 6.3.2.2 Temperature Dependence of $K_D$ and $k_H$ from 273.15 K to $T_c$

The asymptotic relations, given by Eqs. (6.9)–(6.10), should serve as foundations for the equations for $k_H$ and $K_D$ covering the whole temperature range of the vapor–liquid equilibrium for water, from 273.15 to the critical temperature of water, $T_c = 647.096$ K (Wagner and Pruß 2002). After some trials, the following forms were selected for the regression of $K_D$ and $k_H$ data from Table 6.1:

$$RT\ \ln K_D = A_{\mathrm{Kr}}\cdot\frac{2\left(\rho_1^*(L)-\rho_c\right)}{\rho_c^2}\cdot\left\{1 + a_1\,(1-T/T_c) + a_2\,(1-T/T_c)^2\right\}, \tag{6.12}$$

and

$$RT\ \ln\frac{k_H}{f_1^*} = C_o + A_{\mathrm{Kr}}\cdot\frac{\left(\rho_1^*(L)-\rho_c\right)}{\rho_c^2}\cdot\left\{1 + b_1\,(1-T/T_c) + b_2\,(1-T/T_c)^2\right\}, \tag{6.13}$$

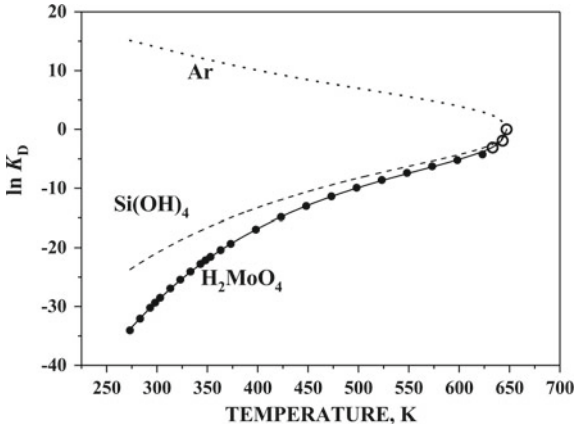


**Fig. 6.3** Temperature dependence of $K_D$: the solid line—Eq. (6.12) for $H_2MoO_4$, solid circles—values from Table 6.1 at 273–623 K, empty circles—values evaluated from the asymptotic relation (6.9) data at 633.15, 643.15 and $T_c$. The dashed and dotted lines show the corresponding dependences for $Si(OH)_4$ (Plyasunov 2012) and Ar (Fernández-Prini et al. 2003)

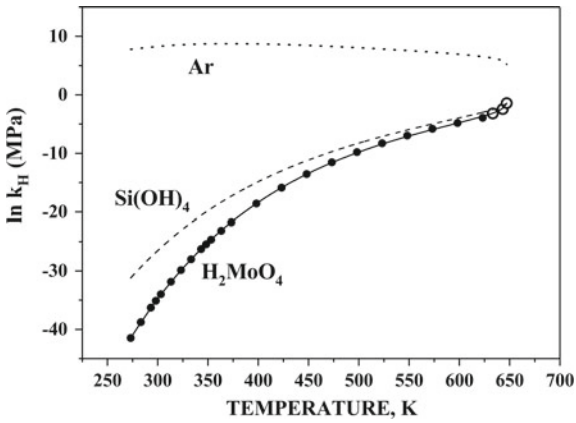


**Fig. 6.4** Temperature dependence of $k_H$. The legend is the same in Fig. 6.3

where the Krichevskii parameter $A_{Kr} = -228$ MPa; $a_1 = -0.373912$, $a_2 = 1.93796$; the constant $C_o = -21{,}980$ J mol$^{-1}$, $b_1 = -0.516457$, $b_2 = 4.06929$. The fitted values of $K_D$ and $k_H$ are shown in Figs. 6.3 and 6.4. The combination of $G^o(g)$ and $k_H$ allowed evaluating $G_2^\infty$ for $H_2MoO_4$ at 633.15, 643.15 and $T_c$, see the corresponding column of Table 6.1.

#### 6.3.2.3 Comparison with Literature Data for Mo and Some Other Solutes

A comparison of $K_D$ values recommended in this study, and those reported in the literature (Khitarov et al. 1967; Rempel et al. 2009; Kokh et al. 2016) is not straightforward. Indeed, the literature partition values are reported as stoichiometric distribution constants, i.e. as ratios of analytical concentrations of elements in coexisting

phases. However, as briefly discussed in Sect. 6.1, the partitioning solute is a non-charged species, $H_2MoO_4$ in the case of Mo(VI) solutions, and its concentration is a strong function of pH of the liquid solution. Nonetheless, a semi-quantitative estimation of $K_D$ values in terms of $H_2MoO_4$ concentrations in coexisting vapor and liquid phases at 623 K based on data of Khitarov et al. (1967), Rempel et al. (2009), Kokh et al. (2016) was undertaken in Dadze et al. (2017a). It was found that the difference with the experimental results (Khitarov et al. 1967; Rempel et al. 2009) exceeded 8 and ~3 orders of magnitude, respectively. By contrast, a relatively close agreement (0.5–1 $\log_{10}$ units) was found with vapor phase concentrations measured by Kokh et al. (2016). Considering a complicated composition of the liquid phase in experiments of Kokh et al. (2016)—0.5 m NaCl, 0.5 m KCl, 0.1 m HCl, 0.01 m $ZnCl_2$, 0.01 m CuCl, 0.01 m $Na_2MoO_4$, plus solid phases $SnO_2$, $SiO_2$, $Fe_2O_3$, $Fe_3O_4$, Pt, Au and simplifications in calculations, this level of agreement appears to be as good as it gets. We remind that Kokh et al. (2016) applied a direct sampling of the coexisting vapor and liquid phases, while Khitarov et al. (1967) and Rempel et al. (2009) attempted to trap a portion of a vapor phase in a two-phase system, which appears to be an error-prone method.

As was discussed in Sect. 6.1, Henry's constants of $H_2MoO_4$ reported in Rempel et al. (2009) exceed those for Ar. According to Fig. 6.4, this result appears grossly in error. Previously we (Dadze et al. 2017a) suggested that $Si(OH)_4$ would be a good proxy for $H_2MoO_4$. As Figs. 6.3 and 6.4 show this is a better, but still not a perfect approximation for $H_2MoO_4$.

## 6.4 Conclusions

Experimental results of the solubility of $MoO_3$ in acid aqueous solutions at 563–623 K were used to determine the thermodynamic properties of the neutral molybdic acid $H_2MoO_4$ at these temperatures (Dadze et al. 2017a). The joint treatment of our own and literature data resulted in a recommendation of the thermodynamic properties of this species at 273–623 K and the saturated water vapor pressure (Dadze et al. 2018a). Combining the Gibbs energies of $H_2MoO_4$ in the state of the aqueous solution with those in the ideal gas state (Akinfiev and Plyasunov 2013), we calculated Henry's constants and the vapor–liquid distribution constants of $H_2MoO_4$ at 273–623 K, and with the use of the relevant asymptotic relations (Japas and Levelt Sengers 1989) extrapolated values of $K_D$ and $k_H$ toward the critical point of pure water. Our results show that over the whole temperature range of existence of the vapor–liquid equilibrium of water, the neutral molybdic acid $H_2MoO_4$ is somewhat less volatile compared with $Si(OH)_4$, and that the difference in volatility of these species decreases with the temperature, see Figs. 6.3 and 6.4.

Finally, we note that many vapor–liquid partitioning results in the geochemical literature are reported as ratios of analytical concentrations of elements in coexisting phases, often having multicomponent compositions. The rigorous thermodynamic

treatment of such data is usually not possible, leaving such results suitable for semi-quantitative modeling at best (or littering the literature with improbable thermodynamic values at worst). If the quantitative modeling of geochemical processes is a goal, even a remote one, than the experimental investigation of the simplest systems, which are easiest for rigorous thermodynamic interpretation, will be of value.

**Acknowledgements** This research was partially supported by the Russian Foundation for Basic Research (Grant # 15-05-2255). The authors thank A. N. Nekrasov and T. N. Dokina (IEM RAS) for SEM and XRD measurements and Dr. V. K. Karandashev (IPTM RAS) for ICP-MS analyses.

## References

Abdulagatov IM, Azizov ND (2003) High-temperature and high pressure densities of aqueous $NaClO_4$ solutions. High Temp High Press 35–36:477–498

Akinfiev AN, Plyasunov AV (2013) Steam solubilities of solid $MoO_3$, ZnO and $Cu_2O$, calculated on a basis of a thermodynamic model. Fluid Phase Equilib 338:232–244

Alvarez J, Corti HR, Fernández-Prini R, Japas ML (1994) Distribution of solutes between coexisting steam and water. Geochim Cosmochim Acta 58(13):2789–2798

Archer DG (1992) Thermodynamic properties of the NaCl + $H_2O$ system. II. Thermodynamic properties of NaCl(aq), NaCl·$2H_2O$(cr), and phase equilibria. J Phys Chem Ref Data 21(4):793–829

Borg S, Liu W, Etschmann B, Tian Y, Brugger J (2012) An XAS study of molybdenum speciation in hydrothermal chloride solutions from 25–385°C and 600 bar. Geochim Cosmochim Acta 92:292–307

Cruywagen JJ (2000) Protonation, oligomerization, and condensation reactions of vanadate(V), molybdate(VI), and tungstate(VI). Adv Inorg Chem 49:127–182

Dadze TP, Kashirtseva GA (2004) Solubility and occurrence mode of gold in acid sulfide solutions. Dokl Earth Sci 395(2):235–237

Dadze TP, Sorokin VI (1986) Solubility of $SnO_2$ in water at 200–400°C and 1.6–150 MPa. Dokl Akad Nauk SSSR 286(2):426–428 (in Russian)

Dadze TP, Sorokin VI, Nekrasov IYa (1981) Solubility of $SnO_2$ in water and in aqueous solutions of HCl, HCl + KCl, and $HNO_3$ at 200–400°C and 1013 bar. Geochem Int 18(5):142–152

Dadze TP, Akhmedzhanova GM, Kashirtseva GA, Orlov PYu (1999) The Au solubility in $H_2S$-bearing aqueous solutions at 300°C. Dokl Earth Sci 369A(9):1275–1276

Dadze TP, Kashirtseva GA, Ryzhenko BN (2000) Gold solubility and species in aqueous sulfide solutions at T = 300°C. Geochem Int 38(7):708–712

Dadze TP, Akhmedzhanova GM, Kashirtseva GA, Orlov PYu (2001) Solubility of gold in sulfide-containing aqueous solutions at T = 300°C. J Mol Liquids 91(1):99–102

Dadze TP, Kashirtseva GA, Novikov MP, Plyasunov AV (2017a) Solubility of $MoO_3$ in acid solutions and vapor-liquid distribution of molybdic acid. Fluid Phase Equilib 440:64–76

Dadze TP, Kashirtseva GA, Novikov MP, Plyasunov AV (2017b) Solubility of $MoO_3$ in $NaClO_4$ solutions at 573 K. J Chem Eng Data 62(11):3848–3853

Dadze TP, Kashirtseva GA, Novikov MP, Plyasunov AV (2018a) Solubility of calcium molybdate in aqueous solutions at 573 K and thermodynamics of monomer hydrolysis of Mo(VI) at elevated temperatures. Monatsh Chem/Chem Month 149(2):261–282

Dadze TP, Kashirtseva GA, Novikov MP, Plyasunov AV (2018b) Solubility of $MoO_3$ in aqueous acid chloride-bearing solutions at 573 K. J Chem Eng Data 63(5):1827–1832

Fernández-Prini R, Alvarez JL, Harvey AH (2003) Henry's constants and vapor–liquid distribution constants for gaseous solutes in $H_2O$ and $D_2O$ at high temperatures. J Phys Chem Ref Data 32(3):903–916

Gorbachev NS, Dadze TP, Kashirtseva GA, Kunts AF (2010) Fluid transfer of gold, palladium, and rare earth elements and genesis of ore occurrences in the Subpolar Urals. Geol Ore Deposit 52(3):215–233

Henderson MP, Miasek VI, Swaddle TW (1971) Kinetics of thermal decomposition of aqueous perchloric acid. Can J Chem 49(2):317–324

Japas ML, Levelt Sengers JMH (1989) Gas solubility and Henry's law near the solvent's critical point. AIChE J 35(5):705–713

Khitarov NI, Arutyunyan LA, Malinin SD (1967) On the possibilities of molybdenum migration in the vapor phase above molybdate solutions at elevated temperatures. Geokhimiya 2:155–159 (in Russian)

Kokh MA, Lopez M, Gisquet P, Lanzanova A, Candaudap F, Besson P, Pokrovski GS (2016) Combined effect of carbon dioxide and sulfur on vapor-liquid partitioning of metals in hydrothermal systems. Geochim Cosmochim Acta 187:311–333

Kudrin AV (1985) The solubility of tugarinovite $MoO_2$ in aqueous solutions at 300–450°C. Geochem Int 22(9):126–138

Kudrin AV (1989) Behavior of Mo in aqueous NaCl and KCl solutions at 300–450°C. Geochem Int 26(8):87–99

Levelt Sengers JMH (1991) Solubility near the solvent's critical point. J Supercrit Fluids 4(4):215–222

Marchenko Z (1971) Photometric determination of elements. Mir, Moscow, 501 p (in Russian)

Palmer DA, Simonson JM, Jensen JP (2004) Partitioning of electrolytes to steam and their solubilities in steam. In: Palmer DA, Fernàndez-Prini R, Harvey AH (eds) Aqueous systems at elevated temperatures and pressures. Elsevier, New York, pp 409–439

Plyasunov AV (2012) Thermodynamics of $Si(OH)_4$ in the vapor phase of water: Henry's and vapor–liquid distribution constants, fugacity and cross virial coefficients. Geochim Cosmochim Acta 77:215–231

Plyasunov AV, Grenthe I (1994) The temperature dependence of stability constant for the formation of polynuclear cationic complexes. Geochim Cosmochim Acta 58(17):3561–3582

Plyasunov AV, Ivanov IP (1991) The solubility of zinc oxide in sodium chloride solutions up to 600°C and 1000 bar. Geochem Int 28(6):77–90

Plyasunov AV, Plyasunova NV (1993a) Study of solubility of zinc oxide in KOH solutions at 400–500°C and pressure 0.5–2.0 kbar. Dokl Akad Nauk SSSR 328(5):605–608 (in Russian)

Plyasunov AV, Plyasunova NV (1993b) Study of solubility of zinc oxide in KOH + NaCl solutions at 400–500°C and pressure 0.5–2.0 kbar. Dokl Akad Nauk SSSR 329(2):228–231 (in Russian)

Plyasunov AV, Belonozhko AB, Ivanov IP, Khodakovsky IL (1988) Solubility of zinc oxide in alkaline solutions at 200–350°C under saturated steam pressure. Geochem Int 25(10):77–85

Rempel KU, Williams-Jones AE, Migdisov AA (2009) The partitioning of molybdenum(VI) between aqueous liquid and vapour at temperatures up to 370°C. Geochim Cosmochim Acta 73(11):3381–3392

Shvarov YuV (2015) A suite of programs, OptimA, OptimB, OptimC, and OptimS compatible with the Unitherm database, for deriving the thermodynamic properties of aqueous species from solubility, potentiometry and spectroscopy measurements. Appl Geochem 55:17–27

Sorokin VI, Dadze TP (1980) Solubility of amorphous $SiO_2$ in water and in aqueous solutions of HCl and $HNO_3$ at temperatures 100–400°C and pressure of 101.3 MPa. Dokl Akad Nauk SSSR 254(3):735–739 (in Russian)

Wagner W, Pruß A (2002) The IAPWS formulation for the thermodynamic properties of ordinary water substance for general and scientific use. J Phys Chem Ref Data 31(2):387–535

Zakirov IV, Dadze TP, Sretenskaya NG, Kashirtseva GA (2008) Experimental data on gold solubility in low-density hydrothermal fluids. Dokl Earth Sci 423(2):1492–1494

Zakirov IV, Dadze TP, Sretenskaya NG, Kashirtseva GA, Volchenkova VL (2009) Gold solubility in low-density fluids in the Au–$H_2O$–$H_2S$–Cl system: experimental data. Geochem Int 47(3):311–314